Title

Three individually addressable spin qubits in a single molecule



Journal

Chemical Communications, 58(54)

ISSN

1359-7345

Authors

Borilovic, Ivana

Roubeau, Olivier

Le Guennic, Boris

et al.

Publication Date

2022-07-05

DOI

10.1039/d2cc02495k

# Three Individually Addressable Spin Qubits in a Single Molecule

Ivana Borilovic,[a] Olivier Roubeau,[b] Boris Le Guennic,[c] Joris van Slageren,[d] Samuel Lenz,[d] Simon J. Teat[e] and Guillem Aromí*[a]

**An asymmetric *bis*-phenol-β-diketone ($H_4L$) has been designed as ligand programmed to promote the assembly of a molecular arrangement composed of three magnetic-exchanged [NiCu] pairs, each exhibiting an $S$ = ½ spin. The latter are shown by EPR and magnetometry to be good qubit realizations, and non-equivalent within the molecule in the solid state, as required for conditional quantum gates.**

The implementation of quantum computing (QC) has recently become an important stimulus for synthetic coordination chemistry research.[1-3] The reason is that the electronic spin has emerged as a promising candidate to embody the two-level quantum systems necessary for the realization of qubits.[4-7] QC aims at realizing algorithms through the coherent manipulation and transfer of the information encoded in qubit quantum states.[8] Molecular spin-based qubits are well-positioned in terms of scalability since they are perfectly reproducible and can be massively prepared, while they benefit from the unlimited versatility of chemical design. Much of the efforts made so far have focused on understanding and maximizing the lifetime or quantum coherence of the qubit quantum states.[9-14] But synthetic chemistry also allows the customized hosting of several spins within molecules for the implementation of multi-qubit quantum gates. However, only few reports address the challenge of making operative molecular quantum gates by engaging more than one qubit. One example is the coupling of pairs of [$Cr_7Ni$] ($S$ = ½ ground state) ring molecular clusters.[15] Coupled vanadyl-based qubits within molecules have also been recently explored as two-qubit quantum gates.[16, 17] Another avenue has been the interplay of two or more non-equivalent lanthanide ions in order to exploit their ground state spin projections ($S_{eff}$ = ½) for the realization of quantum logic gates.[18-21] Some of the molecular devices recently reported incorporate mechanisms for externally gating the coupling between two qubits of a molecule, either by pulsing an electric potential,[22] or through radiation.[23] We have previously reported that *m*-phenylene-spaced phenol-β-diketone units constitute a reliable platform for fixing within individual molecules, pairs of strongly coupled [NiCu] fragments ($S$ = ½), as good realizations of qubits.[24] The similar donor set β,δ-trisketone, separated by an *o*-phenylene was shown to mediate the formation of molecules containing three equivalent [NiCu] pairs,[25] however, no physical characterization was reported. Ensuring non-equivalence of the qubits within a multi-qubit quantum gate is essential for implementing conditional operations. To realize this with molecules of three qubits, we have designed the new ligand 1-methoxy-2,5-*bis*-(3-oxo-3-(2-hydroxyphenyl)-propanoyl)-benzene ($H_4L$, Fig. 1), exhibiting two phenol-β-diketone groups spaced by a methoxide substituted *p*-phenylene. The substituent breaks the symmetry of the ligand, rendering both *bis*-chelating pockets inequivalent. This donor gives access to the predicted molecular coordination cluster [$Ni_3Cu_3(L1)_3(py)_9$] (**1**). The assembly features three inequivalent [NiCu] qubits as a result of the asymmetry engineered on $H_4L$.

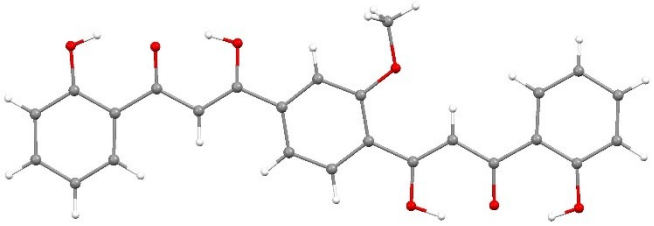

**Figure 1.** Molecular structure of $H_4L$. Color code: O, red; C, grey; H, white.

$H_4L$ was obtained through the Claisen condensation of 2-methoxy-dimethyl terephthalate with two equivalents of 2-hydroxyacetophenone in the same manner as seen previously with a *meta*-phenylene spaced analogue.[26] The di-ester was obtained from the corresponding terephthalic acid, in turn obtained by oxidation of 2,5-dimethylanisole with $KMnO_4$ (Scheme S1). The identity and purity of $H_4L$ was established by microanalysis, mass spectrometry (MS) (Fig. S1) and $^1$H-NMR (Fig. S2). The latter technique confirmed the asymmetric nature of the molecule and also a strong shift of the keto-enolic equilibria towards the enolic forms in both β-diketone groups. The structure determined by SCXRD (Tables S1-S3) shows the fully enolic form also in the solid state (Fig. 1) favoured by intramolecular hydrogen bonds. In the lattice, each ligand interacts with two congeners at opposite sides via two sets of four triangular hydrogen bonds, forming flat ribbons (Fig. S3 and S4) that stack *via* Van der Waals contacts.

$H_4L$ was expected to assemble three pairs of metals disposed as the three bisectors of a triangle (Scheme I) by coordinating their equatorial positions,[25] with the advantage that mixing Ni(II) and Cu(II) should lead exclusively to [NiCu] fragments.[23, 24] A crucial question is whether the methoxide substituents of the methylene spacer lead to three inequivalent qubits or not.

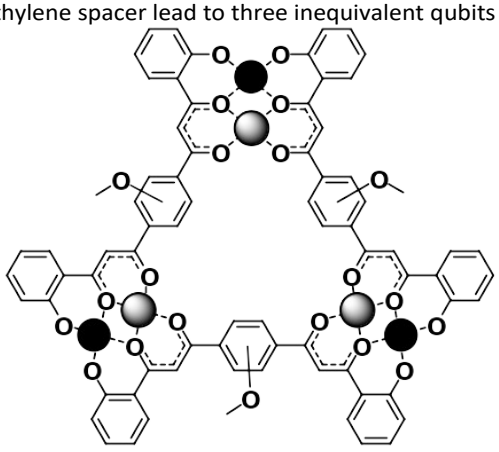

**Scheme I.** Designed structure of the assembly of $L^{4-}$ with a stoichiometric mixture of Ni(II) -grey- and Cu(II) -black- ions.

The reaction of equimolar amounts of $H_4L$, $Ni(ClO_4)_2$ and $Cu(ClO_4)_2$ in pyridine, with excess $Bu_4NOH$, yields the complex [$Ni_3Cu_3(L)_3(py)_9$] (**1**), showing the architecture delineated in Scheme I, according to the balanced equation (1).

$$3\ H_4L + 3\ Ni(ClO_4)_2 + 3\ Cu(ClO_4)_2 + 12\ Bu_4NOH + 9\ py \rightarrow$$
$$\rightarrow [Ni_3Cu_3(L)_3(py)_9] + 12\ Bu_4NClO_4 + 12\ H_2O \quad (1)$$

This compound is stable in solution as shown by MS (Figs. S5 and S6) and EPR measurements (see below). Both techniques

show unequivocally that in the bulk it constitutes a crystalline homogeneous phase with molecules made of three [NiCu] groups, excluding any other distribution of metal ions. The molecular structure of **1** was determined by SCXRD (Tables S1 and S4). The lattice is described by the triclinic $P\bar{1}$ space group with the asymmetric unit containing one formula unit in addition to seven molecules of pyridine. The unit cell is composed of two asymmetric units.

The main complex (Fig. 2 and S7) is a flat cluster of three Cu(II) and three Ni(II) ions assembled by the coordination of all their equatorial positions by three completely deprotonated $L^{4-}$ ligands, *via* all their oxygen atoms in a chelating manner. The three ligands are disposed approximately along the sides of a quasi-equilateral triangle. The metals are distributed as three heterometallic [NiCu] groups, each exhibiting two alkoxo-like bridges. As predicted, the metal ions of the three pairs delineate the bisectors of the molecular triangle, the Ni(II) centres occupying the internal positions while Cu(II) lying at the peripheral sites. Distorted octahedral coordination around the Ni(II) ions is reached through binding of two pyridine ligands on axial positions. Each Cu(II) exhibits square pyramidal geometry, with only one axial pyridine ligand, the latter pointing in one case to the opposite direction than in the other two. In the solid state, this renders two [NiCu] groups inequivalent to the third one. Most importantly, the molecular structure confirms that the asymmetry incorporated into $H_4L$ by a methoxy group on the phenylene spacer makes the three [NiCu] moieties of each molecule of **1** chemically inequivalent. Thus, one [NiCu] metal pair sees two methoxy groups nearby, another pair has one substituent near and another away, whereas the third one has both methoxy groups away (Fig. 2). Despite this, the complex shows quite regular Ni···Cu separations (spanning 3.032 to 3.054 Å) while the intramolecular Ni···Ni distances range 10.157 to 10.325 Å. The molecules of $[Ni_3Cu_3(L)_3(py)_9]$ (**1**) are organized in parallel sheets oriented approximately as the idealized molecular planes and interact mutually by interdigitating the axial pyridine ligands (Fig. S8). Within the sheets, each molecule is surrounded by six congeners (Fig. S9), interacting through an array of weak C–H···O contacts.

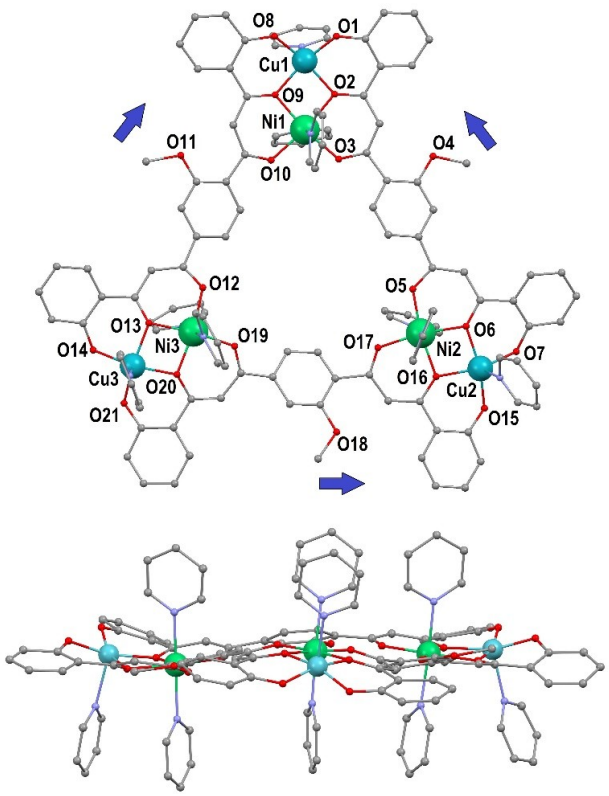


**Figure 2.** Two views of the structure of $[Ni_3Cu_3(L)_3(py)_9]$ (**1**) with non-C and N atoms labelled, the top one showing with arrows the orientation of the –OMe groups that render each [NiCu] fragment inequivalent. H atoms not shown.

A crucial requirement for the [NiCu] units in **1** to be considered as qubit realizations is that they exhibit well-isolated spin doublets (*ie.* the states $|0\rangle$ and $|1\rangle$). In order to realize 3-qubit quantum gates, the qubits must interact weakly to allow for mutual entanglement. These requirements were assessed by bulk magnetization measurements and EPR spectroscopy. The $\chi T$ product of **1** is 3.84 $cm^3Kmol^{-1}$ at 300 K but already shows a decreasing trend upon cooling to reach a plateau at approximately 1.35-1.40 $cm^3Kmol^{-1}$ below 50 K, before featuring a small decline around 7 K down to 1.26 $cm^3Kmol^{-1}$ at 2 K (Fig. 3). The decline at high temperatures indicates a moderate antiferromagnetic interaction between the $Ni^{2+}$ ($S$ = 1) and $Cu^{2+}$ ($S$ = ½) ions within each NiCu pair, while the observation of a plateau confirms the population of the resulting exchange-coupled S = ½ state over a relatively wide range of temperatures. In agreement with this, the solid-state continuous-wave (CW) EPR spectrum recorded at X-band and $T$ = 15 K shows a single line at g = 2.206 (Fig. 3 right), while the magnetization *vs.* field data at 2 K perfectly follows the Brillouin function for this same $g$ value (inset in Fig. 3 left). The EPR spectrum shows no sign of significant anisotropy nor hyperfine splitting, which is likely due to the Cu-Ni exchange interaction dominating the $Ni^{2+}$ ion anisotropy and hyperfine splittings of both $Cu^{2+}$ and $Ni^{2+}$ centers. Also, and in agreement with the plateau in $\chi T$, there is no sign of coupling among the NiCu pairs at $T$ = 15 K. The lower temperature decline of $\chi T$ may be caused by weak intra- or inter-molecular antiferromagnetic interactions between the doublets, and/or the magnetic anisotropy of the Ni(II) single-ion.

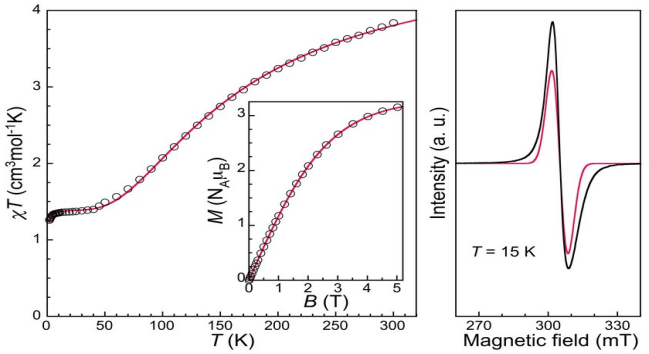


**Figure 3.** Left: $\chi T$ *vs.* $T$ plot of $[Ni_3Cu_3(L)_3(py)_9]$ (**1**). The solid line is a fit (see text) to the experimental data (black circles) collected under a field of 0.5 T. Inset: magnetization vs. field data measured at 2 K. The red line is the Brillouin function at this temperature for a spin 1/2 with g = 2.20. Right: CW-EPR spectrum obtained at X-band (9.418 MHz) and $T$ = 15 K for a polycrystalline sample of **1**. The red line is the spectrum calculated with Easyspin[27] for $S$ = 1/2 , $g_{eff}$ = 2.206 and 6.5 mT Gaussian line broadening.

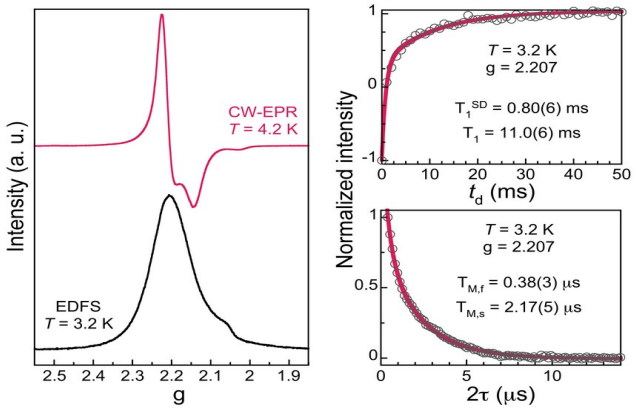


**Figure 4.** (Left) Frozen solution CW (top, X band) and echo detected (bottom, Q band) EPR of **1** at the indicated temperatures. (Right) Inversion recovery (top) and Hahn-echo decay (bottom) of the spin resonance of **1** (see legend).

The magnetic susceptibility data is well reproduced considering unique $J_{Cu-¿}$ = −60.8(5) $cm^{-1}$, $g_{Cu}$ = 2.13(1), $g_{¿}$ = 2.21(1) and mean-field inter-NiCu interaction $zJ'$ = −0.22(2) $cm^{-1}$ (see SI for details). The Ni···Cu coupling observed here lies near the midpoint of the wide range of values (−11.8 to −130 $cm^{-1}$) reported for the scarce examples of this structural moiety (*ie.* the [Cu(μ-O)$_2$Ni] core).[23, 24, 28-37] Among these, no correlation is found between the coupling and the Ni···Cu distance or the Cu−O−Ni angle, but the angle between the metals equatorial planes seems to play a larger role, since it affects the efficiency of the exchange *via* the $d_{x^2-y^2}$ orbitals, leading to stronger coupling with larger co-planarity. The most likely mode of magnetic coupling among the NiCu pairs is through-space and therefore dipolar. A crude estimation based on point-dipole approximation gives a dipolar interaction ceiling of *ca.* 1.6x$10^{-3}$ $cm^{-1}$ (see SI for details), similar to that in a divanadyl 2-qubit system.[16] This small value explains that the EPR spectra show no sign of coupling. Therefore, the mean-field term $zJ'$ is over-estimating the interaction among the NiCu pairs, probably because it also incorporates the effect of the magnetic anisotropy. The ensemble supports the presence of three NiCu units with $S$ = ½ ground states, well-isolated from the quartet state at low temperature and coupled through very weak interactions. Resolution of the asymmetry of these three potential qubits is however prevented by the random orientation of these in bulk samples. Attempts to corroborate the configuration of ligands $L^{4-}$ in **1** observed in the solid state (see above) were made through DFT calculations (Computational details in ESI). While energetic difference is extremely tiny (1 kcal/mol), DFT optimizations indicate that the observed arrangement in solid state indeed is slightly more stable than the symmetric one.

The spin dynamics of the potential qubit formed by each NiCu S = ½ ground state were then studied through pulsed EPR spectroscopy at Q-band. Measurements were performed on a dilute (*ca.* 1 mM) frozen solution of **1** in deuterated THF, to minimize the negative effects on quantum coherence of intermolecular electron spin interactions and interactions with solvent protons nuclear spins. The echo-detected spectrum at 3.2 K is consistent with the X-band CW spectrum obtained for a similar frozen solution of **1** (Fig. 4 left), and both are also consistent with the bulk solid spectrum. This supports the integrity of the [(NiCu)$_3$] complex in solution, in agreement with MS. Inversion recovery and Hahn-echo sequences were then used to determine respectively the spin-lattice relaxation ($T_1$) and phase memory ($T_M$) times, at the main g = 2.207 line and $T$ = 3.2 K. A faster component is observed in both cases, more evident in the inversion recovery data, and the relaxations were thus analyzed as bi-exponential decays (see SI for details). The (slow) spin relaxation time $T_1$ is 11 ms, in line with that previously found in a molecule containing two analogous NiCu pairs (1 ms at 7 K).[23] The fast component estimated as 0.8 ms can reasonably be attributed to spectral diffusion, $T_1^{SD}$, as it is commonly one order of magnitude smaller than $T_1$.[38] The slow/fast components of the phase memory time are 2.17/0.38 μs. The slow component $T_{M,s}$ is relatively long for an exchange-coupled system with non-deuterated organic ligands, compared with other $Cr_7Ni$ and $Cu_3$ qubits previously studied.[13, 39] $T_{M,s}$ is however smaller than that of a molecule containing two analogous NiCu pairs (3.59 μs at 7 K),[23] which could be a consequence of the additional neighboring spin in each [(NiCu)$_3$] complex in **1**.

In summary, the asymmetric ligand $H_4L$ predictively picks Ni(II) and Cu(II) ions from a mixture in solution to deliver a molecular triangular arrangement of three [NiCu] coupled pairs, each exhibiting a well isolated $S$ = ½ spin. The latter are good qubit definitions, as shown through magnetic and EPR (CW and TD) measurements, exhibiting comparatively good quantum coherence. To take advantage of the engineered non-equivalence of these three qubits in the solid state, experiments on (diluted) single crystals will be necessary. Then the three effective $g$ values of the three qubits are distinct, and

selective addressing, also in an ensemble, should be possible. Another possibility, although more challenging experimentally, would be to work on isolated single molecules deposited on the surface of devices.[40]

This research was supported by Spanish MINECO (PGC2018-098630-B-I00, MAT2017-86826-R), the Aragón government (E31_20R PLATON) and the EU (FET-OPEN grant 862893 FATMOLS). G. A. thanks the Generalitat de Catalunya for the prize ICREA Academia 2018. B.L.G. thanks French GENCI/IDRIS-CINES centers for high-performance computing resources. The authors thank the Advanced Light Source, which is a DOE Office of Science User Facility under contract no. DEAC02-05CH11231 and the Zeiss Foundation for funding.

## References

1. E. J. L. McInnes, G. A. Timco, G. F. S. Whitehead and R. E. P. Winpenny, *Angew. Chem., Int. Ed.*, 2015, **54**, 14244-14269.
2. G. Aromí, D. Aguilà, P. Gamez, F. Luis and O. Roubeau, *Chem. Soc. Rev.*, 2012, **41**, 537-546.
3. A. Gaita-Ariño, F. Luis, S. Hill and E. Coronado, *Nature Chem.*, 2019, **11**, 301-309.
4. A. Ardavan and S. J. Blundell, *J. Mater. Chem.*, 2009, **19**, 1754-1760.
5. P. C. E. Stamp and A. Gaita-Arino, *J. Mater. Chem.*, 2009, **19**, 1718-1730.
6. M. J. Martinez-Perez, S. Cardona-Serra, C. Schlegel, F. Moro, P. J. Alonso, H. Prima-Garcia, J. M. Clemente-Juan, M. Evangelisti, A. Gaita-Arino, J. Sese, J. van Slageren, E. Coronado and F. Luis, *Phys. Rev. Lett.*, 2012, **108**, 247213.
7. G. Aromí, F. Luis and O. Roubeau, in *Lanthanides and Actinides in Molecular Magnetism*, eds. R. A. Layfield and M. Murugesu, Wiley-WCH, 2015, ch7, pp. 185-221.
8. M. A. Nielsen and I. L. Chuang, *Quantum Computation and Quantum Information*, Cambridge University Press, 2000.
9. S. Lenz, K. Bader, H. Bamberger and J. van Slageren, *Chem. Commun.*, 2017, **53**, 4477-4480.
10. K. Bader, D. Dengler, S. Lenz, B. Endeward, S. D. Jiang, P. Neugebauer and J. van Slageren, *Nature Commun.*, 2014, **5**, 6304.
11. M. J. Graham, C.-J. Yu, M. D. Krzyaniak, M. R. Wasielewski and D. E. Freedman, *J. Am. Chem. Soc.*, 2017, **139**, 3196-3201.
12. K. S. Pedersen, A.-M. Ariciu, S. McAdams, H. Weihe, J. Bendix, F. Tuna and S. Piligkos, *J. Am. Chem. Soc.*, 2016, **138**, 5801-5804.
13. C. J. Wedge, G. A. Timco, E. T. Spielberg, R. E. George, F. Tuna, S. Rigby, E. J. L. McInnes, R. E. P. Winpenny, S. J. Blundell and A. Ardavan, *Phys. Rev. Lett.*, 2012, **108**, 107204.
14. M. Atzori, E. Morra, L. Tesi, A. Albino, M. Chiesa, L. Sorace and R. Sessoli, *J. Am. Chem. Soc.*, 2016, **138**, 11234-11244.
15. S. J. Lockyer, S. Nawaz, A. Brookfield, A. J. Fielding, I. J. Vitorica-Yrezabal, G. A. Timco, N. A. Burton, A. M. Bowen, R. E. P. Winpenny and E. J. L. McInnes, *J. Am. Chem. Soc.*, 2020, **142**, 15941-15949.
16. I. Borilovic, P. J. Alonso, O. Roubeau and G. Aromí, *Chem. Commun.*, 2020, **56**, 3139-3142.
17. M. Atzori, A. Chiesa, E. Morra, M. Chiesa, L. Sorace, S. Carretta and R. Sessoli, *Chem. Sci.*, 2018, **9**, 6183-6192.
18. D. Aguilà, L. A. Barrios, V. Velasco, O. Roubeau, A. Repollés, P. J. Alonso, J. Sesé, S. J. Teat, F. Luis and G. Aromí, *J. Am. Chem. Soc.*, 2014, **136**, 14215-14222.
19. F. Luis, A. Repolles, M. J. Martinez-Perez, D. Aguila, O. Roubeau, D. Zueco, P. J. Alonso, M. Evangelisti, A. Camon, J. Sese, L. A. Barrios and G. Aromi, *Phys. Rev. Lett.*, 2011, **107**.
20. Y. H. Lan, S. Klyatskaya, M. Ruben, O. Fuhr, W. Wernsdorfer, A. Candini, V. Corradini, A. L. Rizzini, U. del Pennino, F. Troiani, L. Joly, D. Klar, H. Wende and M. Affronte, *J. Mater. Chem., C*, 2015, **3**, 9794-9801.
21. E. Macaluso, M. Rubín, D. Aguilà, A. Chiesa, L. A. Barrios, J. I. Martínez, P. J. Alonso, O. Roubeau, F. Luis, G. Aromí and S. Carretta, *Chem. Sci.*, 2020, **11**, 10337-10343.
22. J. Ferrando-Soria, E. M. Pineda, A. Chiesa, A. Fernandez, S. A. Magee, S. Carretta, P. Santini, I. J. Vitorica-Yrezabal, F. Tuna, G. A. Timco, E. J. L. McInnes and R. E. P. Winpenny, *Nature Commun.*, 2016, **7**, 11377.
23. J. Salinas-Uber, M. Estrader, J. Garcia, P. Lloyd-Williams, A. Sadurni, D. Dengler, J. van Slageren, N. F. Chilton, O. Roubeau, S. J. Teat, J. Ribas-Arino and G. Aromi, *Chem., Eur. J.*, 2017, **23**, 13648-13659.
24. L. A. Barrios, D. Aguila, O. Roubeau, P. Gamez, J. Ribas-Arino, S. J. Teat and G. Aromi, *Chem., Eur. J.*, 2009, **15**, 11235-11243.
25. F. Li, J. K. Clegg, P. Jensen, K. Fisher, L. F. Lindoy, G. V. Meehan, B. Moubaraki and K. S. Murray, *Angew. Chem., Int. Ed.*, 2009, **48**, 7059-7063.
26. G. Aromí, C. Boldron, P. Gamez, O. Roubeau, H. Kooijman, A. L. Spek, H. Stoeckli-Evans, J. Ribas and J. Reedijk, *Dalton Trans.*, 2004, 3586-3592.
27. S. Stoll and A. Schweiger, *J. Magn. Reson.*, 2006, **178**, 42-55.
28. Z.-X. Zhu, L.-Z. Cai, X.-W. Deng, Y.-L. Zhou and M.-X. Yao, *New J. Chem.*, 2017, **41**, 11097-11103.
29. I. Morgenstern-Badarau, M. Rerat, O. Kahn, J. Jaud and J. Galy, *Inorg. Chem.*, 1982, **21**, 3050-3059.
30. Y. Journaux, O. Kahn, I. Morgenstern-Badarau, J. Galy, J. Jaud, A. Bencini and D. Gatteschi, 1985, **107**, 6305-6312.
31. C. N. Verani, E. Rentschler, T. Weyhermüller, E. Bill and P. Chaudhuri, *J. Chem. Soc., Dalton Trans.*, 2000, 251-258.
32. M. Yonemura, M. Ohba, K. Takahashi, H. Ōkawa and D. E. Fenton, *Inorg. Chim. Acta*, 1998, **283**, 72-79.
33. C. J. O'Connor, D. P. Freyberg and E. Sinn, 1979, **18**, 1077-1088.
34. Y. Sunatsuki, T. Matsuo, M. Nakamura, F. Kai, N. Matsumoto and J.-P. Tuchagues, *Bull. Chem. Soc. Jpn.*, 1998, **71**, 2611-2619.
35. M. Yonemura, K. Arimura, K. Inoue, N. Usuki, M. Ohba and H. Ōkawa, *Inorg. Chem.*, 2002, **41**, 582-589.
36. A. Hori, Y. Mitsuka, M. Ohba and H. Ōkawa, *Inorg. Chim. Acta*, 2002, **337**, 113-121.
37. T. Aono, H. Wada, Y.-I. Aratake, N. Matsumoto, H. Ōkawa and Y. Matsuda, *J. Chem. Soc., Dalton Trans.*, 1996, 25-29.
38. S. S. Eaton and G. R. Eaton, in *Biological Magnetic Resonance*, ed. L. J. Berliner, Kluwer Academic / Plenum Publishers, New York, 2000, vol. 19.
39. P. Lutz, R. Marx, D. Dengler, A. Kromer and J. van Slageren, *Mol. Phys.*, 2013, **111**, 2897-2902.
40. M. D. Jenkins, D. Zueco, O. Roubeau, G. Aromí, J. Majer and F. Luis, *Dalton Trans.*, 2016, **45**, 16682-16693.